

# Space-Time Behavior of Single and Bimanual Rhythmical Movements: Data and Limit Cycle Model

B. A. Kay

J. A. S. Kelso

E. L. Saltzman

G. Schöner

# Space-Time Behavior of Single and Bimanual Rhythmical Movements: Data and Limit Cycle Model

B. A. Kay

University of Connecticut and Haskins Laboratories,  
New Haven, Connecticut

E. L. Saltzman

Haskins Laboratories, New Haven, Connecticut and  
University of Connecticut

J. A. S. Kelso

Center for Complex Systems, Florida Atlantic University and  
Haskins Laboratories, New Haven, Connecticut

G. Schöner

Center for Complex Systems, Florida Atlantic University

How do space and time relate in rhythmical tasks that require the limbs to move singly or together in various modes of coordination? And what kind of minimal theoretical model could account for the observed data? Earlier findings for human cyclical movements were consistent with a nonlinear, limit cycle oscillator model (Kelso, Holt, Rubin, & Kugler, 1981) although no detailed modeling was performed at that time. In the present study, kinematic data were sampled at 200 samples/second, and a detailed analysis of movement amplitude, frequency, peak velocity, and relative phase (for the bimanual modes, in phase and antiphase) was performed. As frequency was scaled from 1 to 6 Hz (in steps of 1 Hz) using a pacing metronome, amplitude dropped inversely and peak velocity increased. Within a frequency condition, the movement's amplitude scaled directly with its peak velocity. These diverse kinematic behaviors were modeled explicitly in terms of low-dimensional (nonlinear) dissipative dynamics, with linear stiffness as the *only* control parameter. Data and model are shown to compare favorably. The abstract, dynamical model offers a unified treatment of a number of fundamental aspects of movement coordination and control.

How do space and time relate in rhythmical tasks that require the hands to move singly or together in various modes of coordination? And what kind of minimal theoretical model could account for the observed data? The present article addresses these fundamental questions that are of longstanding interest to experimental psychology and movement science (e.g., von Holst, 1937/1973; Scripture, 1899; Stetson & Bouman, 1935). It is well known, for example, that discrete and repetitive movements of different amplitude vary systematically in movement duration (provided accuracy requirements are held constant, e.g., Craik, 1947a, 1947b). This and related facts were later formalized into Fitts's Law (1954), a relation among movement time, movement amplitude, and target accuracy, whose underpinnings have been extensively studied (and debated upon) quite recently (e.g., Meyer, Smith, & Wright, 1982; Schmidt, Zelaznik, Hawkins, Frank, & Quinn, 1979).

In the present study, the accuracy of movement is neither fixed nor manipulated as in many investigations of Fitts's Law:

Only frequency is scaled systematically and amplitude allowed to vary in a natural way. Surprisingly, there has been little research on movements performed under these particular experimental conditions (see Freund, 1983). Feldman (1980) reported data from a subject who attempted to keep a *maximum* amplitude (elbow angular displacement) as frequency was gradually increased to a limiting value (7.1 Hz). An observed inverse relation was accompanied by an increasing tonic coactivation of antagonistic muscles. In addition, the slope of the so-called "invariant characteristic" (see also Asatryan & Feldman, 1965; Davis & Kelso, 1982)—a plot of joint torque versus joint angle—increased with rhythmical rate, suggesting that natural frequency (or its dynamic equivalent, stiffness) was a controllable parameter. Other studies have scaled frequency but fixed movement amplitude. Their conclusions were similar to Feldman's: Frequency changes over a range were accounted for by an increase in system stiffness (e.g., Viviani, Soechting, & Terzuolo, 1976).

---

Work on this article was supported by National Institute of Neurological and Communicative Disorders and Stroke Grant NS-13617, Biomedical Research Support Grant RR-05596, and Contract N0014-83-K-0083 from the U.S. Office of Naval Research. G. Schöner was supported by a Forschungsstipendium of the Deutsche Forschungsgemeinschaft, Bonn.

Thanks to David Ostry, John Scholz, Howard Zelaznik, and three anonymous reviewers for comments.

Correspondence concerning this article should be addressed to J. A. S. Kelso, Center for Complex Systems, P.O. Box 3091, Florida Atlantic University, Boca Raton, Florida 33432.

Brooks and colleagues (e.g., Conrad & Brooks, 1974; see Brooks, 1979, for review) used a rather different paradigm for exploring spatiotemporal relations in cyclic movement patterns. In several studies, monkeys produced rapid elbow flexions/extensions as they slammed a manipulandum back and forth between mechanical stops (thus allowing no variation in amplitude). After a training period, the movement amplitudes were shortened artificially by bringing the stops closer together. The monkeys, however, continued to exert muscular control for the "same" length of time, pressing the handle against the stops when they would normally have produced larger amplitude movements. Because the original rhythm of

rapid alterations established during training was maintained in the closer-stop condition, "the rhythm . . . or some correlate of it" (Brooks, 1979, p. 23) was deemed to be centrally programmed. However, it is not at all clear how these findings or conclusions relate to situations in which subjects are not prevented from adjusting movement amplitude voluntarily in response to scalar increases in rate (see Schmidt, 1985).

With regard to less confined experimental paradigms in which speech and handwriting have been studied, several interesting results have come to light. As speaking rate is increased, for example, the displacement of observed articulator movements is reduced (e.g., Kelso, Vatikiotis-Bateson, Saltzman, & Kay, 1985; Kent & Moll, 1972, Ostry & Munhall, 1985). The precise nature of the function relating these variables, however, is not known because only a few speaking rates have been employed in such experiments. In handwriting, it is well known that when the amplitude of the produced letter is increased, movement duration remains approximately constant (e.g., Hollerbach, 1981; Katz, 1948; Viviani & Terzuolo, 1980). This handwriting result is theoretically interesting in at least two respects. First, many interacting degrees of freedom are involved in writing a letter, be it large or small, yet quite simple kinematic relations are reproducibly observed at the end effector. Second, because the anatomy and biomechanics are entirely different between writing on notepaper and on a blackboard, a rather abstract control structure is implicated.

In the present article we offer a dynamical model that is entirely consistent with such an abstract control structure and that is shown to reproduce observed space-time relations of limbs operating singly or together (in two specific modes of coordination) quite nicely. Moreover, exactly the same model can be applied to *transitions* among coordinative modes of hand movement (see below). The present dynamical model is not tied locally and concretely to the biomechanics of the musculoskeletal periphery. Rather, the approach is consistent with an older view of dynamics, namely, that it is the *simplest and most abstract* description of the motion of a system (Maxwell, 1877/1952, p. 1). It is possible to use such abstract dynamics in complex multidegree of freedom systems when structure or patterned forms of motion arise (e.g., Haken, 1975, 1983). Such patterned regularities in space and time are characterized by low-dimensional dynamics whose variables are called *order parameters*. One can imagine, for example, the high dimensionality involved in a simple finger movement were one to include a description of participating neurons, muscles, vascular processes, and so forth, along with their interconnections. Yet in tasks such as pointing a finger, the whole ensemble cooperates in such a way that it can be described by a simple, damped mass-spring dynamics for the end effector position. Thus, under the particular boundary conditions set by the pointing task, end position and velocity are the order parameters that fully specify the cooperative behavior of the ensemble. Such "compression," from a microscopic basis of huge dimensionality to a macroscopic, low-dimensional structure, is a general and predominant feature of nonequilibrium, open systems (e.g., Haken, 1983). In the context of movement, this reduction of degrees of freedom is characteristic of a coordinative structure, namely, a functional grouping of many neuromuscular components that are

flexibly assembled as a single, functional unit (e.g., Kelso, Tuller, Vatikiotis-Bateson, & Fowler, 1984).

In earlier work (e.g., Kelso, Holt, Kugler, & Turvey, 1980; Kugler, Kelso, & Turvey, 1980), we have identified such unitary ensembles—following Feldman (1966)—with the qualitative behavior of a damped mass-spring system. Such systems possess a *point attractor*; that is, all trajectories converge to an asymptotic, static equilibrium state. Thus, the property of *equifinality* is exhibited, namely, a tendency to achieve an equilibrium state regardless of initial conditions. The control structure for such motion can be characterized by a set of time-independent dynamic parameters (e.g., stiffness, damping, equilibrium position), with kinematic variations (e.g., position, velocity, acceleration over time) emerging as a consequence. This dynamical model has received a broad base of empirical support from studies of single, discrete head movement (Bizzi, Polit, & Morasso, 1976), limb movement (e.g., Cooke, 1980; Polit & Bizzi, 1978; Schmidt & McGown, 1980) and finger-movement targeting tasks (Kelso, 1977; Kelso & Holt, 1980). In addition, point attractor dynamics can be shown to apply not only to the muscle-joint level but also to the abstract, task level of description as well (see Saltzman & Kelso, 1987). That is, a dynamical description is appropriate at more than one "level." Striking support for this notion has been recently accumulated by Hogan and colleagues (see Hogan, 1985). In their work on postural maintenance of the upper extremity, the well known "spring-like" behavior of a single muscle was shown to be a property of the entire neuromuscular system. As Hogan (1985) notes, ". . . despite the evident complexity of the neuromuscular system, coordinative structures . . . go to some length to preserve the simple 'spring-like' behavior of the single muscle at the level of the complete neuromuscular system" (p. 166).

It is important to emphasize that point attractor dynamics provide a *single* account of both posture and targeting movements. Hence, a shift in the equilibrium position (corresponding to a given postural configuration) gives rise to movement (see e.g., Feldman, 1986). What, then, of rhythmical movement, our major concern here? It is easy to see, in principle, how a dynamical description might be elaborated to include this case. For example, a single movement to a target may be underdamped, overdamped, or critically damped, depending on the system's parameter values (for example, see Kelso & Holt, 1980). A simple way to make the system oscillate would be to change the sign of the damping coefficient to a negative value. This amounts to inserting "energy"<sup>1</sup> into the system. However, for the motion to be bounded, an additional dissipative mechanism must be present in order to balance the energy input and produce stable limit cycle motion. This combination of linear negative damping and nonlinear dissipative components comprises an *escapement* function for the system that is *autonomous* in the conventional mathematical sense of a time-independent forcing function.

In the present research we adopt this autonomous description of rhythmical movement, though we do not exclude—on em-

<sup>1</sup> It is important to emphasize here that we use terms like *energy* and *dissipation* in the abstract sense of dynamical systems theory (cf. Jordan & Smith, 1977; Minorsky, 1962). These need not correspond to any observable biomechanical quantities.

pirical grounds alone—the possibility that forcing may occur in a time-dependent fashion. Oscillator theory tells us that *nonlinear* autonomous systems can possess a so-called *periodic attractor* or limit cycle; that is, all trajectories converge to a single cyclic orbit in the phase plane ( $x, \dot{x}$ ). Thus, a nontrivial feature of both periodic attractor dynamics and rhythmical movement (entirely analogous to the foregoing discussion of point attractor dynamics and discrete movement) is stability in spite of perturbations and different initial conditions.

In a set of experiments several years ago, we demonstrated such orbital stability (along with other behaviors such as mutual and subharmonic entrainment) in studies of human cyclical movements (Kelso, Holt, Rubin, & Kugler, 1981). Although our data were consistent with a nonlinear limit cycle oscillator model for both single and coupled rhythmic behavior, no explicit attempt to model the results was made at that time. More recently, however, Haken, Kelso, and Bunz (1985) have successfully modeled the circumstances under which observed transitions occur between two modes of coupling the hands—namely, antiphase motion of relative phase  $\approx 180^\circ$ , which involves nonhomologous muscle groups, and in-phase motion of relative phase  $\approx 0^\circ$ , in which homologous muscles are used. The Haken et al. (1985) nonlinearly coupled nonlinear oscillator model was able to reproduce the phase transition, that is, the change in qualitative behavior from antiphase to in-phase coordination that occurs at a critical driving frequency, as the driving frequency ( $\omega$ ) was continuously scaled (see Kelso, 1981, 1984; MacKenzie & Patla, 1983). This model has been further extended in a quantitative fashion to reveal the crucial role of relative phase fluctuations in provoking observed changes in behavioral pattern between the hands and to further identify the phenomenon as a nonequilibrium phase transition (Schöner, Haken, & Kelso, 1986). Remarkably good agreement between Schöner et al.'s (1986) stochastic theory and experiments conducted by Kelso and Scholz (1985) and Kelso, Scholz, and Schöner (1986) has been found.

In the present work we provide quantitative experimental results pertinent to the foregoing modeling work of Haken et al. (1985) and Schöner et al. (1986). For example, although the Haken et al. (1985) model provided a qualitative account of decreases in hand movement amplitudes with increasing frequency, the actual function relating these variables was not empirically measured in earlier experiments nor was any fit of parameters performed. A goal of this research is to show how a rather simple dynamical model (or control structure)—requiring variations in only one system parameter—can account for the spatiotemporal behavior of the limbs acting singly and together. The experimental strategy was to have subjects perform cyclical movements in response to a metronome whose frequency was manipulated (in 1-Hz steps) between 1 Hz and 6 Hz. The data reveal a stable and reproducible reciprocal relation between cycling frequency and amplitude for both single and bimanual movements. This constraint between the spatial and temporal aspects of movement patterns invokes immediately a nonlinear dynamical model (linear systems exhibit no such constraint), the particular parameters of which can be specified according to kinematic observables (e.g., frequency, amplitude, and maximum velocity). Though we make no claims for the uniqueness of the present model, we do show that

other models can be excluded by the data, and we suggest explicit ways in which uniqueness may be sought.

## Method

### Subjects

The subjects were 4 right-handed male volunteers, none of whom were paid for their services. They individually participated in two experimental sessions, which were separated by a week. Each session consisted of approximately 1 hr of actual data collection.

### Apparatus

The apparatus was a modification of one described in detail on previous occasions (Kelso & Holt, 1980; Kelso et al., 1981). Essentially, it consisted of two freely rotating hand manipulanda that allowed flexion and extension about the wrist (radiocarpal) joint in the horizontal plane. Angular displacement of the hands was measured by two DC potentiometers riding the shafts of the wrist positioners. The outputs of the potentiometers and a pacing metronome (see below) were recorded with a 16-track FM tape recorder (EMI SE-7000).

### Procedure

Subjects were placed in a dentist's chair, their forearms rigidly placed in the wrist-positioning device, so that the wrist joint axes were directly in line with the positioners' vertical axes. Motion of the two hands was thus solely in the horizontal plane. Vision of the hands was not excluded.

Each experimental session was divided into two subsessions. In the first session, single-handed movements were recorded, followed by two-handed movements; this was reversed for the second session. Within each subsession, preferred movements were recorded, followed by metronome-paced movements. For the preferred trials, subjects were told to move their wrists cyclically "at a comfortable rate." On the paced trials, subjects were told to follow the "beeps" of an audio metronome to produce one full cycle of motion for each beep. Pacing was provided for six different frequencies—1, 2, 3, 4, 5, and 6 Hz—presented in random order. For both the preferred and paced conditions, subjects were not instructed explicitly concerning the amplitude of movement; for example, they were not told to move their wrists maximally.

For the single-hand subsession there were, therefore, 14 conditions, one preferred and six paced data sets being collected for each hand. For the two-handed trials, there were also 14 conditions, one preferred and six paced data sets being collected for each of two different movement patterns. These bimanual patterns consisted of a mirror, symmetric mode, which involved the simultaneous activation of homologous muscles and a parallel, asymmetric mode, which involved simultaneous activation of nonhomologous muscle groups (see, e.g., Kelso, 1984). Two trials of data were collected for each condition in each session. For the preferred trials, 30 s of data were collected, while 20 s were collected at the pacing frequencies of 1–4 Hz, and 6 s–8 s at 5 Hz and 6 Hz, to minimize fatigue effects.

### Data Reduction and Dependent Measures

Following the experimental sessions, the movement signals were digitized at 200 samples/second and smoothed with a 35-ms triangular window. Instantaneous angular velocity was computed from the smoothed displacement data by means of the two-point central difference algorithm and smoothed with the same triangular window (see Kay, Munnhall, Vatikiotis-Bateson, & Kelso, 1985, for details of the signal processing steps involved). A cycle was defined by the occurrence of two (adja-

Table 1  
*Mean Frequency, Amplitude, and Peak Velocity for Single-Handed Trials*

Condition	Frequency (Hz)				Amplitude (degrees)				Peak velocity (degrees/second)			
	Left		Right		Left		Right		Left		Right	
	<i>M</i>	%	<i>M</i>	%	<i>M</i>	%	<i>M</i>	%	<i>M</i>	%	<i>M</i>	%
Preferred Paced	2.04	3.8	2.04	3.3	46.87	7.2	46.88	6.4	311.91	6.5	307.08	6.1
1 Hz	1.00	6.9	1.00	4.9	51.17	5.8	53.54	7.0	194.04	8.5	187.40	8.7
2 Hz	2.00	3.7	2.00	3.3	43.11	7.6	46.01	7.7	291.19	8.2	298.62	7.8
3 Hz	3.00	4.7	3.00	4.0	37.74	10.7	40.50	8.1	358.17	9.4	380.45	7.0
4 Hz	4.02	6.5	4.04	4.8	38.64	10.7	33.54	10.7	463.31	9.0	416.85	8.6
5 Hz	5.19	7.8	5.14	4.9	32.82	13.7	33.35	9.6	540.37	9.8	522.10	7.6
6 Hz	6.33	6.9	6.01	6.6	26.81	21.8	27.83	12.9	516.89	10.9	499.33	10.7

Note. Means are collapsed across trials, sessions, and subjects. Percentages represent average within-trial cross-cycle coefficients of variation.

cent) peak extension events, which, along with peak flexions, were identified by a peak-peaking algorithm. Peak velocity was measured using the same peak picker on the velocity data; the values reported here are summaries across both positive and negative velocity peaks. Cycle frequency (in Hz) was defined as the inverse of the time between two peak extensions, and cycle amplitude (peak-to-peak, in degrees) as the average of the extension-flexion, flexion-extension half-cycle excursions. For the two-handed trials, the relative phase (or phase difference) between the two hands was also computed on a cycle-by-cycle basis, using Yamanishi, Kawato, and Suzuki's (1979) definition. This is a purely temporal measure and is not computed from a motion's phase plane trajectory (Kelso & Tuller, 1985). The measurement is based on the temporal location of a left peak extension within a cycle of right-hand movement as defined above. In our convention, for the mirror mode, phase differences of less than 0° indicate that the left hand leads the right, and vice versa for positive values. For the parallel, asymmetric mode, values of less than 180° mean that the left hand leads the right (i.e., the left peak extension event is reached prior to exactly 180°); values greater than 180° mean that the right hand leads. For qualitative comparisons between model-generated simulations and data, phase plane trajectories were also examined. These were created by simultaneously plotting transduced angular position against the derived instantaneous velocity.

After obtaining these measures for each cycle, we obtained measures of central tendency (means) and variability across all cycles of each trial.

Coefficients of variation (CVs) were used as variability measures for frequency, amplitude, and peak velocity to remove the effects of the frequency scaling on the mean data and thus to validly compare variability data across the observed frequency range. The standard deviation was used as the phase variability measure, because coefficients of variation would be clearly inappropriate in comparing the two patterns of movement, whose mean phase differences were always around 0° and 180°. In the following Results section are reported these within-trial summary data, because of the large number of cycles collected. In under 1% of the trials, a trial was lost because of experimenter error. Thus, for statistical purposes, means across trials within each experimental condition were used.

## Results

The means and variability measures of frequency (in Hz), amplitude (in degrees), peak velocity (in degrees/second) and relative phase (for the two-handed conditions) are presented in Tables 1 to 4, collapsed across trials, sessions, and subjects. Both preferred and paced data are included in these tables.

### *Preferred Conditions Frequency, Amplitude, and Peak Velocity*

For both single and bimanual preferred movements, repeated measures analyses of variance (ANOVAs) were performed on the

Table 2  
*Mean Frequency, Amplitude, and Peak Velocity for Homologous (Mirror) Two-Handed Trials*

Condition	Frequency (Hz)				Amplitude (degrees)				Peak velocity (degrees/second)			
	Left		Right		Left		Right		Left		Right	
	<i>M</i>	%	<i>M</i>	%	<i>M</i>	%	<i>M</i>	%	<i>M</i>	%	<i>M</i>	%
Preferred Paced	1.90	7.3	1.90	6.6	41.49	4.0	47.05	3.7	252.93	7.3	280.72	6.6
1 Hz	1.00	3.9	1.00	4.0	52.71	6.2	56.85	6.0	188.30	8.6	196.60	8.2
2 Hz	2.00	3.5	2.00	3.3	38.80	9.6	42.20	8.1	260.85	9.4	280.91	7.5
3 Hz	3.01	5.3	3.00	4.0	33.15	11.0	35.85	9.6	318.45	9.4	345.51	8.1
4 Hz	4.08	8.1	4.08	5.7	30.50	14.1	32.95	11.6	387.18	9.5	415.44	9.0
5 Hz	5.29	9.7	5.25	5.5	26.12	17.6	29.64	13.5	430.64	12.4	474.90	11.2

Note. Means are collapsed across trials, sessions, and subjects only for the stable data. Percentages show average within-trial, cross-cycle coefficients of variation.

Table 3  
*Mean Frequency, Amplitude, and Peak Velocity for Nonhomologous (Parallel) Two-Handed Trials*

Condition	Frequency (Hz)				Amplitude (degrees)				Peak velocity (degrees/second)			
	Left		Right		Left		Right		Left		Right	
	<i>M</i>	%	<i>M</i>	%	<i>M</i>	%	<i>M</i>	%	<i>M</i>	%	<i>M</i>	%
Preferred Paced	1.56	3.8	1.56	4.1	52.30	5.7	57.50	4.7	288.57	6.8	314.39	4.9
1 Hz	1.01	4.2	1.01	3.9	53.22	6.5	54.79	5.7	196.21	9.3	201.96	7.7
2 Hz	2.02	4.4	2.00	3.8	46.41	9.3	48.21	7.7	316.15	7.8	325.46	7.3

Note. Means are collapsed across trials, sessions, and subjects only for the stable data. Percentages represent average within-trial, cross-cycle coefficients of variation.

within-trial means, and variability measures were obtained for frequency, amplitude, and peak velocity. The design was a  $2 \times 3 \times 2$  factorial, with hand (left, right), movement condition (single, mirror, and parallel), and session as factors.

*Mean data.* Looking first at frequency means, the only effect found was for movement condition,  $F(2, 6) = 9.14, p < .05$ . Post hoc Scheffé tests show that in the single (2.04 Hz) and mirror (1.90 Hz) mode the preferred frequencies were similar to each other but higher than in the parallel mode frequency (1.56 Hz). The two hands did not differ in preferred frequency in any of the three movement conditions. With regard to amplitude means, a main effect for hand,  $F(1, 3) = 14.16, p < .05$ , and a Hand  $\times$  Mode interaction,  $F(2, 6) = 5.81, p < .05$ , occurred. There was no significant movement condition effect, suggesting that the three movement conditions assumed the same amplitude in the preferred case. However, the interaction indicated that the amplitude means for the single conditions were identical for the two hands but differed in both bimanual conditions, the left hand assuming a lower amplitude than the right in each case. No significant main effects or interactions were found for the preferred peak velocity data.

*Variability data.* ANOVAs performed on the frequency and peak velocity within-trial coefficients of variation revealed no

effects. For the amplitude CVs, however, there was a significant effect for movement condition,  $F(2, 6) = 5.17, p < .05$ . Post hoc tests showed that single-hand amplitudes were more variable than parallel amplitudes, which were more variable than those for mirror movements.

### Relative Phase

For the bimanual movement conditions, repeated measures ANOVAs were performed on the within-trial means and standard deviations of the relative phase between the two hands. The design was a  $2 \times 2$  factorial, Coordinative Mode (mirror and parallel)  $\times$  Session. The only effect observed for phase was mode,  $F(1, 3) = 13756.6, p < .0001$ , showing that the subjects were indeed performing the task properly, producing two distinct phase relations between the hands. The 95% confidence interval for the mirror mode was  $6.56^\circ \pm 11.34^\circ$ , and for the parallel mode,  $185.28^\circ \pm 9.93^\circ$ ; the intervals overlap with the "pure" modes of  $0^\circ$  and  $180^\circ$ , respectively (although in both modes the right hand tends to lead the left). There were no effects or interactions for phase variability in the preferred conditions.

### Metronome-Paced Conditions

As can be seen in Tables 1–4, the manipulation of movement frequency had a profound effect on almost all the measured observables. With increasing frequency, amplitude decreased, whereas peak velocity and all variability measures appeared to increase. There were some apparent differences among the three movement conditions as well, although the two hands behaved quite similarly. Valid comparisons among the experimental conditions on the kinematic variables of frequency, amplitude, and peak velocity can be made, however, only when it is established that subjects are actually performing the bimanual tasks in a stable fashion. Looking at Table 4, one can see that the phase variability of the two modes increased quite rapidly with increasing frequency.

In a  $6 \times 2 \times 2$  factorial design, with pacing frequency (1–6 Hz in 1-Hz steps), coordinative mode (mirror and parallel), and session as factors, the only effect observed on the mean relative phase data was mode,  $F(1, 3) = 233.01, p < .001$ , and the means observed across all pacing frequencies were  $4.21^\circ$  and  $182.93^\circ$

Table 4  
*Mean Relative Phase for Homologous (Mirror) and Nonhomologous (Parallel) Two-Handed Trials*

Condition	Relative phase (degrees)			
	Homologous		Nonhomologous	
	<i>M</i>	<i>SD</i>	<i>M</i>	<i>SD</i>
Preferred Paced	6.46	11.36	185.28	11.09
1 Hz	3.60	6.75	177.75	9.54
2 Hz	10.44	10.84	185.99	16.65
3 Hz	6.19	18.00	188.82	52.49
4 Hz	4.00	26.36	193.64	93.46
5 Hz	-5.81	42.53	181.68	104.02
6 Hz	5.33	51.91	168.88	110.38

Note. Means (*M*) are collapsed across trials, sessions, and subjects. Standard deviations (*SD*) are average within-trial, cross-cycle *SD*s.

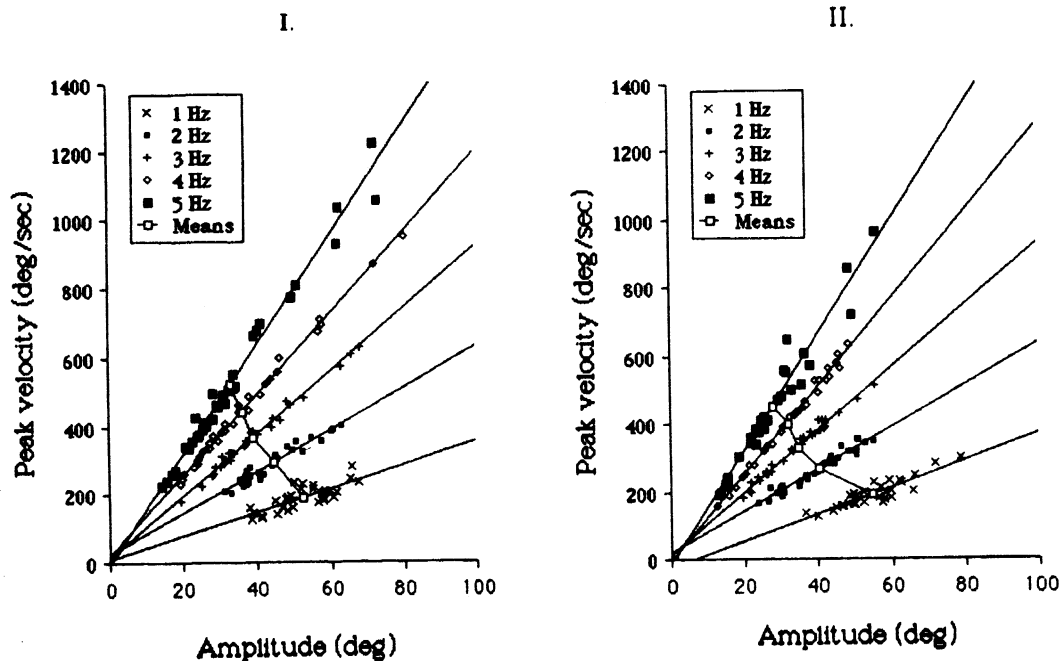


Figure 1. Amplitude (in degrees) and peak-velocity (in degrees/second) individual trial data for the 1–5 Hz pacing frequencies, and means within each frequency. Left panel: single-handed movements. Right panel: mirror-mode movements.

in the mirror and parallel modes, respectively. Apparently the two criterion phase angles are approximated, *on the average*, within trials. However, effects for pacing frequency,  $F(5, 15) = 124.91, p < .0001$ , mode,  $F(1, 3) = 265.75, p < .001$ , and their interaction,  $F(5, 15) = 18.24, p < .001$ , were found on the within-trial relative phase standard deviations. The interaction was consistent with both main effects: Variability in phase increased with increasing frequency for both modes, but the parallel mode's variability increased much faster than the mirror mode's. Note, in Table 4, the order of magnitude increase in phase variability in the parallel mode between 2 Hz and 3 Hz. A comparable degree of phase variability in the mirror mode is not evident until the 6-Hz pacing condition. This result is consistent with other findings (e.g., Kelso, 1984; Kelso & Scholz, 1985) that the parallel mode is highly unstable between 2 Hz and 3 Hz for similar movements, and a transition to the mirror mode is frequently observed above that frequency.

The foregoing pattern of phase variability suggests, therefore, that we perform two separate analyses on the remainder of the paced data in order to make comparisons only within the stable regions of behavior. A reasonable criterion for phase stability is  $\pm 45^\circ$ . Thus, we now report (a) the analyses comparing mirror mode and single-hand behavior from 1 Hz to 5 Hz and (b) the analyses on all three movement conditions for 1 Hz and 2 Hz.

#### Single-Hand Versus Mirror-Mode Movements, 1–5 Hz

For single-hand and mirror-mode paced movements, repeated measures ANOVAs were performed on the within-trial means, and variability measures were obtained for frequency, amplitude, and peak velocity. The design was a  $5 \times 2 \times 2 \times 2$

factorial, with pacing frequency (1–5 Hz in 1-Hz steps), hand (left, right), movement condition (single and mirror) and session as factors.

*Mean data.* With regard to the observed frequency means, the pacing frequency was, as expected, a highly significant effect,  $F(4, 12) = 1117.76, p < .0001$ . The only other effect present was a weak three-way interaction, Session  $\times$  Hand  $\times$  Pacing Frequency  $F(4, 12) = 4.51, p < .05$ , indicating some very minor fluctuations in observed frequency. The main feature of this interaction is a simple effect for mode at the 3-Hz pacing frequency,  $F(2, 6) = 9.02, p < .02$ , which was observed for none of the other pacing frequencies.

For the amplitude means, the main effect of pacing frequency,  $F(4, 12) = 9.51, p < .005$ , shows that amplitude decreased with increasing frequency. Three of the 4 subjects' linear correlations between amplitude and frequency were significant, (Pearson  $r_s = -.50, -.86, \text{ and } -.87, p_s < .001$ ), while the 4th subject's amplitude trend, although decreasing, failed to reach significance ( $r = -.18, p = .12$ ). The only other effect on amplitude was a weak three-way interaction, Mode  $\times$  Hand  $\times$  Pacing Frequency,  $F(4, 12) = 3.30, p < .05$ , chiefly the result of the left-hand amplitude in the single case at 5 Hz being slightly higher than the rest of the data at that frequency. Otherwise, no differences were found, the two movement conditions exhibiting much the same amplitude across the entire frequency range. Pacing frequency,  $F(4, 12) = 8.26, p < .005$ , was the only significant effect on the peak velocity means; the latter increased with increasing frequency for both movement conditions.

The main effect of pacing frequency found for both amplitude and peak velocity indicates that each covaries with fre-

quency of movement, but an interesting relation exists between the two: With respect to the means across each pacing frequency, amplitude and peak velocity exhibited an *inverse* relation (see Figure 1) for both the single-hand and mirror movements ( $r = -.986$  for the single hands,  $r = -.958$  for the mirror movements, on the overall means;  $N = 5$  and  $p < .01$  for both correlations). At first, this result seems to contradict a wealth of findings on this relation which reveal that peak velocity scales *directly* with movement amplitude (see Kelso & Kay, in press, for a review). However, an analysis of the individual trial data within a given pacing frequency condition indicates that peak velocity and amplitude do indeed scale directly with each other (see Figure 1). Pearson's  $r$  correlations for each of the movement frequencies are listed in Table 5, and range from .772 to .997 ( $p < .01$  in all cases). Slopes of the lines of best fit for peak velocity as a function of amplitude are also reported; none of the intercepts were significantly different from zero.

**Variability data.** The within-trial coefficients of variation (CVs) for observed frequency showed significant effects of pacing frequency,  $F(4, 12) = 13.68, p < .0005$ ; hand,  $F(1, 3) = 12.59, p < .05$ ; and the Pacing Frequency  $\times$  Mode interaction,  $F(4, 12) = 5.92, p < .01$ . Overall, the left hand was more variable in frequency than the right (CVs of 6.0% and 4.4%, respectively). Analysis of simple main effects showed that pacing frequency was a significant effect for both single-hand and mirror movements,  $F(4, 12) = 3.989, p < .05$ , and  $F(4, 12) = 33.24, p < .0001$ , respectively, but that the only difference between the two movement conditions occurred at 3 Hz,  $F(1, 3) = 20.18, p < .05$ . At that pacing frequency, the mirror mode was slightly more variable than the single-hand movements.

The only significant effect on amplitude CVs was pacing frequency,  $F(4, 12) = 29.10, p < .0001$ . Amplitude variability increased very consistently with increasing movement frequency (see also Figure 1, which shows the cross-trial variability in amplitude as well as in peak velocity). For the peak velocity CVs, session,  $F(1, 3) = 13.10, p < .05$ , and pacing frequency,  $F(4, 12) = 3.51, p < .05$ , were significant effects; variability in the second session was lower than that in the first (the only clear-cut practice effect in the experiment), and higher frequency movements were consistently more variable on this measure.

#### *Comparison of All Three Movement Conditions at 1 Hz and 2 Hz*

For all three movement conditions, repeated measures ANOVAs were performed on the within-trial means, and variability measures were obtained for frequency, amplitude, and peak velocity. The design was a  $2 \times 2 \times 3 \times 2$  factorial, with pacing frequency (1 Hz and 2 Hz), hand (left, right), movement condition (single, mirror, parallel), and session as factors.

**Mean data.** For the observed frequency, pacing frequency,  $F(1, 3) = 32708.6, p < .0001$ , and mode,  $F(1, 3) = 6.64, p < .05$ , were significant effects, with the parallel mode being slightly faster than the other two movement conditions overall. The difference, however, was less than 1% of the pacing frequency. For amplitude, no main effects or interactions were found; the three movement conditions assumed a single overall amplitude, and amplitude differences were not apparent across the two observed frequencies. For peak velocity, pacing fre-

quency,  $F(1, 3) = 19.32, p < .05$ , and its interactions with movement condition,  $F(2, 6) = 5.92, p < .05$ , and hand,  $F(1, 3) = 15.18, p < .05$ , were significant. A simple main effects analysis for the first of these interactions indicated that the pacing frequency effect was significant for the single and parallel movements but not for the mirror mode. In addition, the movement conditions differed at 2 Hz (order from least to greatest peak velocity: mirror, single, parallel) but not at 1 Hz. The second interaction was consistent with the associated main effects—the pacing frequency effect was significant for both hands, and no simple effects for hand appeared. However, at 2 Hz the right hand showed slightly greater peak velocities than the left. As observed for single-hand and mirror movements (see above), amplitude and peak velocity covaried directly in the parallel movements, within each pacing frequency (see Table 5).

**Variability data.** For observed frequency, no main effects or interactions were found for the within-trial CVs. For amplitude CVs, the Movement Condition  $\times$  Hand interaction was significant,  $F(2, 6) = 13.51, p < .05$ , yet no simple main effects were found at any level of the two independent variables. However, for the left hand, both bimanual conditions were more variable than single-hand movements, whereas the reverse was true for the right. For peak velocity CVs, the only effect was a weak three-way interaction of movement condition, hand, and frequency,  $F(2, 6) = 7.87, p < .05$ .

#### *Qualitative Results—Examples of Phase Portraits*

The shapes of the limit cycle trajectories can be very informative about the underlying dynamics. Figure 2 shows typical phase plane trajectories for single-hand movements; a section of one trial is displayed for each of the pacing frequencies from 1 Hz to 6 Hz, along with the trajectories of the model (see next section on limit cycle models) at the same frequencies. As shown in the figure, trajectory shape varies with movement frequency: Higher frequency movements appear to be somewhat more sinusoidal (i.e., more elliptical on the phase plane) than lower frequency ones. This was especially apparent in going from 1 Hz to 2 Hz. Some subjects showed this tendency less than others, but the shapes of the trajectories did not appear to differ among the three movement conditions. Note also that the velocity profiles are unimodal in these rhythmical movements, a result also observed in recent speech (Kelso et al., 1985) and discrete arm movements (e.g., Bizzi & Abend, 1983; Cooke, 1980; Viviani & McCollum, 1983).

#### *Limit Cycle Modeling*

In this section we first present a limit cycle model that accounts for a number of observed kinematic characteristics of rhythmical hand movements, including the observed amplitude–frequency and peak velocity–frequency relations across conditions, as well as the peak velocity–amplitude relation within a given pacing condition. In addition, an adequate generalization of the limit cycle model to coordinated rhythmic hand movements is presented (Haken et al., 1985), and conclusions are drawn from comparisons with the experimental data. A discussion of the assumptions that are implicit in our modeling strategy is deferred to the General Discussion.



Table 5  
Correlations of Amplitude and Peak Velocity, Within Each Pacing Frequency, for Stable Frequencies

Frequency	Condition								
	Single			Mirror			Parallel		
	<i>r</i>	<i>m</i>	<i>N</i>	<i>r</i>	<i>m</i>	<i>N</i>	<i>r</i>	<i>m</i>	<i>N</i>
1 Hz	.772	3.44	32	.903	3.98	30	.733	4.62	26
2 Hz	.970	6.08	32	.972	6.19	32	.967	6.58	32
3 Hz	.995	9.09	32	.992	9.15	32			
4 Hz	.997	11.77	33	.996	12.82	36			
5 Hz	.991	15.94	34	.975	16.86	28			

Note. *r* = Pearson's *r*; *m* = slope of the line of best fit (peak velocity as a function of amplitude); *N* = number of trials for each correlation.

As noted earlier by Haken et al. (1985), a combination of two well-known limit cycle oscillators is a strong candidate to model the observed monotonous decrease of amplitude as a function of frequency. These two oscillators are the van der Pol (van der Pol, 1922) and the Rayleigh oscillator (Rayleigh, 1877/1945). The first is described by an equation of motion of the following form:

$$\ddot{x} + \alpha\dot{x} + \gamma x^2\dot{x} + \omega^2x = 0, \quad (1)$$

where  $\alpha$ ,  $\gamma$ , and  $\omega^2$  are constants. For  $\alpha < 0$  and  $\gamma > 0$ , this equation has a limit cycle attractor. In a phase portrait in the  $(x, \dot{x})$ -plane this means that there is a closed curve on which the system rotates (the limit cycle) and to which all trajectories are attracted after a sufficiently long transient time. For  $|\alpha| \ll \omega$  the frequency of oscillation on and near the limit cycle is, to a good approximation, just  $\omega$  (see Minorsky, 1962, Section 10.6). Figure 3 illustrates this situation schematically.

An analytic description of the limit cycle can be given if the slowly varying amplitude and rotating wave approximations are used (Haken et al., 1985; see Appendix A for a brief summary of the methods and the results). The amplitude of the limit cycle, which in this approximation is a harmonic oscillation, is found to be

$$A = 2\sqrt{|\alpha|/\gamma} \quad (2)$$

and is independent of the frequency  $\omega$ . Thus the van der Pol oscillator can account for the intercept of the amplitude-frequency relation but not for its monotonic decrease. The Rayleigh oscillator has the equation of motion,

$$\ddot{x} + \alpha\dot{x} + \beta\dot{x}^3 + \omega^2x = 0, \quad (3)$$

and possesses a limit cycle attractor for  $\alpha < 0$ ,  $\beta > 0$ , again with an oscillation frequency  $\omega$  as long as  $|\alpha| \ll \omega$ . Using again the two above-mentioned approximations, we obtain the amplitude of this limit cycle as

$$A = (2/\omega)\sqrt{|\alpha|/3\beta} \quad (4)$$

(see Haken et al., 1985).

The decrease of amplitude with frequency observed in the data is captured by this expression, although the divergence of Equation 4 at small frequency is clearly nonphysical.

It is easy to imagine that a combination of both types of oscillators may provide a more accurate account of the experimental results. Therefore, let us consider the following model:

$$\ddot{x} + \alpha\dot{x} + \beta\dot{x}^3 + \gamma x^2\dot{x} + \omega^2x = 0, \quad (5)$$

which we refer to from now on as the "hybrid" oscillator. For  $\beta, \gamma > 0$ ,  $\alpha < 0$  this yields again a limit cycle attractor of frequency  $\omega$  (for  $|\alpha| \ll \omega$ ) with amplitude (again in the approximations of Appendix A):

$$A = 2\sqrt{|\alpha|/(3\beta\omega^2 + \gamma)}. \quad (6)$$

This function exhibits both a hyperbolic decrease in amplitude as well as a finite intercept at zero frequency and accounts qualitatively for the experimental data. In Figure 4 we have plotted the amplitude  $A$  of the hybrid model together with the experimental data as a function of frequency. The two parameters,  $\beta$  and  $\gamma$ , were fitted (using a least squares fit; see Footnote 2) while  $\alpha$  was chosen as  $\alpha = -0.05 \times \omega_{\text{pref}}$  ( $= .641$  Hz) without a further attempt to minimize deviations from the data. (The values for  $\beta$  and  $\gamma$  were  $\beta = .007095$  Hz<sup>3</sup>,  $\gamma = 12.457$  Hz, where  $A$  was taken to be of the same scale as the experimental degree values.) The choice of  $\alpha$  is consistent with the slowly varying amplitude approximation (for which we need  $|\alpha| \ll \omega$ ; see Appendix A) and amounts to assuming that the nonlinearity is weak (see Appendix B and General Discussion below). For illustrative purposes, the corresponding least squares fits for the van der Pol and the Rayleigh oscillators are also shown in Figure 4. Note that only one fit parameter,  $\beta$  or  $\gamma$  respectively, was used for these fits. It is obvious how each of the two foregoing models accounts for only one aspect of the experimental observations, and the hybrid model accounts for both. In summary, the model parameters were determined by (a) identifying the pacing frequency with  $\omega$  (which is a good approximation for  $|\alpha| \ll \omega$ ); (b) choosing  $\alpha = -0.05 \times \omega_{\text{pref}}$ ; and (c) finding  $\beta$  and  $\gamma$  by a least squares fit of the amplitude-frequency relation. A more stringent evaluation of the parameters is possible if more experimental information is available (see the discussion of the assump-

<sup>2</sup> The parameters  $\beta$  and  $\gamma$  were found by means of a pseudo-Gauss-Newton search for the parameters, using the single-hand observed frequency and amplitude trial data ( $N = 192$ ). The least squares criterion was the minimization of squared residuals from the model amplitude-frequency function stated in Equation 6. The overall fit was found to be significant,  $F(2, 190) = 35.314$ ,  $p < .0001$ , and the overall  $R^2$  was .2748; standard deviations for  $\beta$  and  $\gamma$  were .001025 Hz<sup>3</sup> and 1.0129 Hz, respectively.

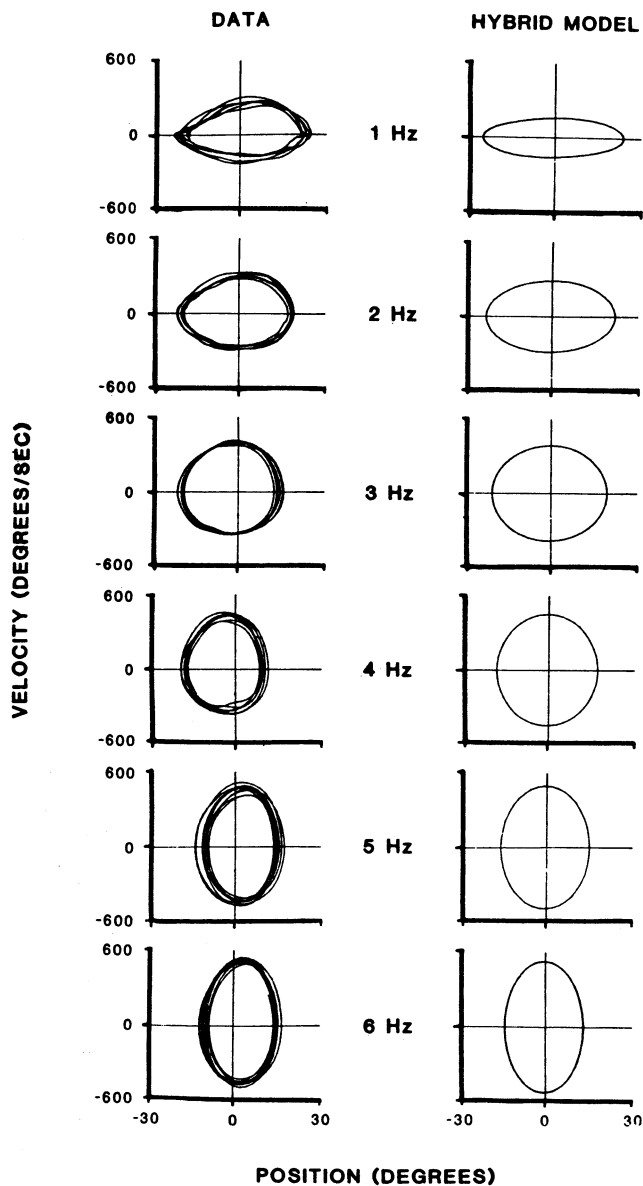


Figure 2. Phase plane trajectories from 1 Hz to 6 Hz. Left panel: representative examples from the collected data set of 1 subject. Right panel: trajectories of the hybrid model (Equation 5), simulated on digital computer.

tions in General Discussion below). Note, however, that even on this level of sophistication the model accommodates several further features of the data. For example the peak velocity–amplitude relation given by the limit cycle model is the simple relation

$$V_p = \omega A. \quad (7)$$

This relation holds whenever the trajectory is close to the limit cycle. Thus if trajectories fluctuate around the limit cycle (due to ever-present small perturbations), we expect the scatter of the peak velocity–amplitude data to lie on a straight line of slope  $\omega$ . Moreover, this same relation is shown to hold in the situation

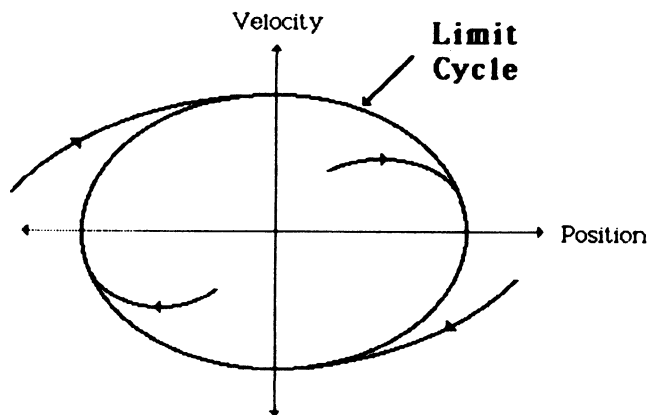


Figure 3. Examples of phase plane trajectories for a limit cycle.

where amplitude varies across trials (see Figure 1 and Table 5). Note that peak-to-peak amplitude equals  $2A$  so that the slopes reported in Table 5 are  $\omega/2 = \pi \times \text{Frequency}$ . An additional piece of experimental information concerns the peak velocity–frequency relation (see Table 1 and Figure 5), the theoretical prediction for which results if we insert Equation 6 into Equation 7 as follows:

$$V_p = 2\omega \sqrt{|\alpha| / (3\beta\omega^2 + \gamma)}. \quad (8)$$

This theoretical curve is also included in Figure 5. It is important to emphasize that all parameters have been fixed previously. Clearly, the match between model and experiment is quite close.

We now turn to the modeling of the two-handed movements. The essential idea is to couple two single-hand oscillators of type expressed in Equation 5. Assuming symmetry of the two hands, Haken et al., (1985) have established the most simple

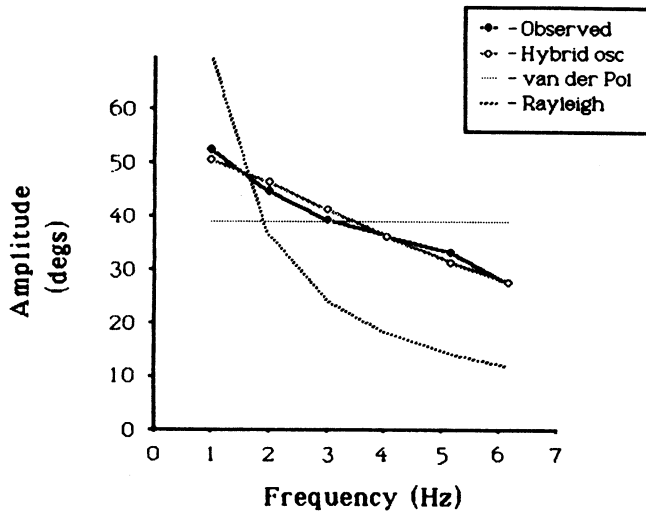


Figure 4. Frequency (in Hz) versus amplitude (in degrees) for the single-handed data and the curves of best fit for the van der Pol, the Rayleigh, and the hybrid oscillators. (The observed data are the mean values at each pacing frequency.)

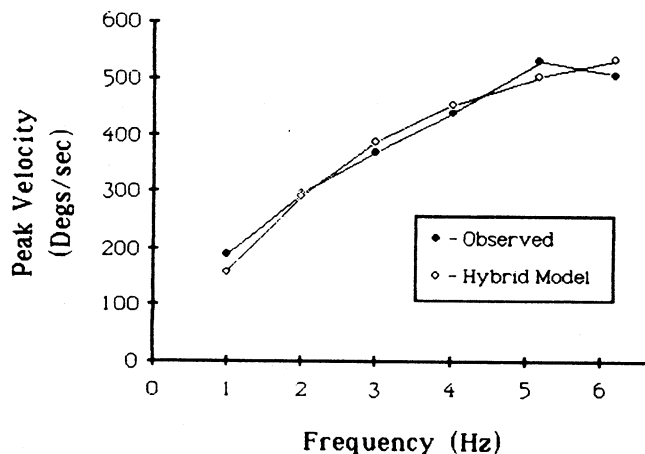


Figure 5. Frequency (in Hz) versus peak velocity (in degrees/second) for the single-handed data and the corresponding function for the hybrid model (see Equation 8), as derived from the amplitude–frequency data. (The observed data are the mean values at each pacing frequency.)

coupling structure that accounts for both the in-phase (symmetric/mirror) and the antiphase (asymmetric/parallel) coordinative modes as well as the transition from an asymmetric to symmetric organization as frequency is scaled (see introduction). This coupling structure has the following explicit form:

$$\ddot{x}_1 + g(x_1, \dot{x}_1) = (\dot{x}_1 - \dot{x}_2)[a + b(x_1 - x_2)^2] \quad (9)$$

$$\ddot{x}_2 + g(x_2, \dot{x}_2) = (\dot{x}_2 - \dot{x}_1)[a + b(x_2 - x_1)^2], \quad (10)$$

where

$$g(x, \dot{x}) = \alpha\dot{x} + \beta\dot{x}^3 + \gamma x^2\dot{x} + \omega^2 x, \quad (11)$$

and  $a$  and  $b$  are coupling constants. Using again the approximations of Appendix A (see Haken et al., 1985, for the calculations), one obtains the amplitudes

$$A_1 = A_2 = 2 \sqrt{\frac{|\alpha| + a(1 - \cos\phi)}{3\beta\omega^2 + \gamma - 3b + 4b\cos\phi - b\cos 2\phi}}. \quad (12)$$

In this expression  $\phi = \phi_2 - \phi_1$  is the relative phase of the two oscillators, which is  $\phi = \pm 180^\circ$  for the asymmetric motion and  $\phi = 0^\circ$  for the symmetric motion. Note that for  $a = b = 0$  we recover the amplitude of the single hybrid oscillator (see Equation 6). Indeed, the experimental observation that the amplitudes of the two-handed modes of movement did not differ significantly from the single-hand amplitudes leads us to the conclusion that the coupling is weak in the sense that  $a \ll \alpha$  and  $b \ll \gamma$ . This is an interesting result in that it shows that even when the coupling is much weaker than the corresponding dissipative terms of the single-hand oscillators (which guarantee a stable amplitude–frequency relation), phase locking and transitions within phase locking can occur. This may rationalize, to some degree, the ubiquity of phase locking in the rhythmical movements of animals and people and is worthy of much more investigation.

A final remark concerns the preferred frequencies chosen by subjects in the single-hand condition compared with the two

coordinative modes. The observation was that the preferred frequency was always lower in the asymmetric mode than in either the symmetric mode or the single-hand movement conditions, which were roughly equal. As mentioned before, a transition takes place from the asymmetric mode to the symmetric mode as frequency is scaled beyond a certain critical value. The coupled oscillator model accounts for that transition in the sense that the stationary state  $\phi \approx \pm 180^\circ$  for the relative phase becomes unstable (Haken et al., 1985). In fact, the stability of that state decreases when frequency increases, as exhibited by the relaxation rate of this state (see Schöner et al., 1986, and General Discussion). A simple analysis reveals that the preferred frequency in the asymmetric mode is shifted in such a way that the stability of the relative phase is larger than it would be if the preferred frequency of the single-hand oscillation were maintained. This observation may well be important for a fuller understanding of the preferred frequencies, in terms, perhaps, of variational principles such as minimization of energy (see Hoyt & Taylor, 1981; Kelso, 1984).

## General Discussion

In this article we have shown how a low-dimensional description in terms of dissipative dynamics can account—in a unified manner—for a number of observed facts. First, the present “hybrid” model includes the well-known mass-spring characteristic of postural tasks (see introduction). That is, when the linear damping coefficient,  $\alpha$ , is positive, the model exhibits a stable equilibrium position in the resting state ( $x = 0, \dot{x} = 0$  is a point attractor). Second, when the sign of the linear damping coefficient is negative, this equilibrium point is unstable, and an oscillatory solution with a frequency determined by the linear restoring force,  $\omega^2 x$ , is stable and attracting. The persistence of the oscillation and its stability is guaranteed by a balance between excitation (via  $\alpha\dot{x}$  with negative damping coefficient,  $\alpha < 0$ ), and dissipation (as indexed by the nonlinear dissipative terms,  $\beta\dot{x}^3$  and  $\gamma x^2\dot{x}$ ). This balance determines the limit cycle, a periodic attractor to which all paths in the phase plane ( $x, \dot{x}$ ) converge from both the inside and the outside. For example, if  $\dot{x}$  or  $x$  are large, corresponding to a condition outside the limit cycle, the dissipative terms dominate and amplitude will decrease. If, on the other hand,  $\dot{x}$  and  $x$  are small, the linear excitation term dominates and amplitude will increase (see Figure 3). Third, oscillatory behavior is systematically modified by specific parameterizations, such as those created by a pacing manipulation. The model accounts for the amplitude–frequency and peak velocity–frequency relations with a simple change in one parameter, the linear stiffness  $\omega^2$  (for unit mass). Further support for the latter control parameter comes from the direct scaling relation (observed *within* a pacing condition) of peak velocity and amplitude—a relation that is now well established in a variety of tasks (e.g., Cooke, 1980; Jeannerod, 1984; Kelso, Southard, & Goodman, 1979; Kelso et al., 1985; Ostry & Munhall, 1985; Viviani & McCollum, 1983). Thus, a number of kinematic characteristics and their relations emerge from the model’s dynamic structure and parameterization. Fourth, and we believe importantly, the same oscillator model for the individual limb behavior can be generalized to the case of coordinated rhythmic action. A suitable coupling of limit cycle (hy-

brid) oscillators gives rise to transitions among modes of coordination when the pacing frequency reaches a critical value (Haken et al., 1985; Kelso & Scholz, 1985; Schöner et al., 1986). Indeed, a number of additional phenomena can now be accommodated, including the “seagull effect” observed by Yamanishi, Kawato, and Suzuki (1980) and Tuller and Kelso (1985; see Kelso, Schöner, Scholz, & Haken, 1987, Section 6).

In summary, the model offers a synthesis of a variety of quite different movement behaviors that we have simulated explicitly on a digital computer (see Figure 2). That is, a successful implementation of the model has been effected that is now subject to further controlled experimentation. One appealing aspect of the model is that it formalizes and extends some of Feldman’s (1966) early but influential work (see, e.g., Bizzi et al., 1976; Cooke, 1980; Kelso, 1977; Ostry & Munhall, 1985; Schmidt & McGown, 1980). Feldman (1966) presented observations on the execution of rhythmic movement that strongly suggested that the nervous system was capable of controlling the natural frequency of the joint using the so-called invariant characteristics—a plot of joint angle versus torque (see also Berkenblit, Feldman, & Fukson, 1986; Davis and Kelso, 1982). But he also recognized that “a certain mechanism to counteract damping in the muscles and the joint” must be brought into play, in order to “make good the energy losses from friction in the system” (Feldman, 1966, p. 774). Our model shows—in an abstract sense—how excitation and dissipation balance each other so that stable rhythmic oscillations may be produced.

On the other hand, in modeling movement in terms of low-dimensional, nonlinear dynamics, we have made certain assumptions that will now be addressed, because they require additional experimental test. For reasons of clarity we list these modeling assumptions systematically.

1. *Equifinality*. This is a pivotal issue of the entire approach. The very fact that the oscillatory movement pattern can be reached reproducibly from uncontrolled initial conditions indicates—as far as the theory is concerned—that (a) a description of the system dynamics in terms of a single variable (a displacement angle about a single rotation axis) and its derivative is sufficient—that is, there are no hidden dynamical variables that influence the movement outcome—and that (b) the modeling in terms of a low-dimensional description must be dissipative in nature (allowing for attractor sets that are reached independent of initial conditions). An experimental test of the equifinality property consists of studying the stability of the movement pattern under perturbations. Although such stability was observed in earlier studies (Kelso et al., 1981), a much more systematic investigation is now required.

2. *Autonomy*. A further reduction in the number of relevant variables is possible through the assumption of autonomous dynamics. Nonautonomous forcing—as mentioned in the introduction—essentially represents one additional variable, namely, time itself. Apart from the conceptual advantages discussed in the introduction, there are experimental ways to test this assumption. One such method consists of studying phase resetting curves in perturbation experiments (Winfree, 1980). For example, in a system driven by a time-dependent forcing function (e.g., a driven damped harmonic oscillator), perturbations will not introduce a permanent phase shift. On the other hand, if consistent phase shifts are observed in the data, the

rhythm cannot be due fundamentally to a nonautonomous driving element.

A strong line of empirical support for the autonomy assumption comes from the transition behavior in the bimanual case, as frequency is scaled (Kelso, 1981, 1984; Kelso & Scholz, 1985). Here autonomous dynamics were able to account for the transition behavior in some detail (Haken et al., 1985; Schöner, et al. 1986). Note also that during the transition one or both of the hands must make a shift in phase, a result that would require a not easily understood change in the periodic forcing function(s); that is, one or both “timing programs” would have to alter in unknown ways to accomplish the transition.

3. *Minimality*. The effective number of system degrees of freedom can be further limited by the requirement that the model be minimal in the following sense: The attractor layout (i.e., the attractors possible for varying model parameters) should include only attractors of the observed type. In the present single-hand case, for example, the model should not contain more than a (monostable) limit cycle and a single fixed point (corresponding to posture). This limits the dynamics to those of second order: Higher orders would allow, for example, quasiperiodic or chaotic solutions (e.g., Haken, 1983), which have not been observed thus far.

The above considerations (equifinality, autonomy, and minimality) thus constrain the number of possible models considerably. Explicitly, the most general form of the model given these constraints is

$$\ddot{x} + f(x, \dot{x}) = 0. \quad (13)$$

We can illustrate the relation of the hybrid model to the general case (Equation 13) by expanding  $f$  in a Taylor series (assuming symmetry under the operation  $x \rightarrow -x$ , as inferred to be a good approximation from the phase portraits [Figure 2]), as follows:

$$\ddot{x} = \omega^2 x + \alpha \dot{x} + \beta \dot{x}^3 + \gamma x^2 \dot{x} + \delta x \dot{x}^2 + \epsilon x^3 + 0(x^5, x\dot{x}^4). \quad (14)$$

The hybrid model (Equation 5) then results from putting  $\delta = \epsilon = 0$ .

Our discussion of modeling assumptions can be drawn to a close by remarking that more detailed information about the system dynamics can now be gained by asking experimental questions that are motivated by the theory. For example, in the model the system’s *relaxation time* (i.e., the time taken to return to the limit cycle after a perturbation) is approximately the inverse of  $\alpha$  (see Appendix A), which a simple dimensional analysis reveals to be related to the strength of the nonlinearity (see Appendix B). Thus, relaxation time measurements can give important information about how and by how much the system supplies and dissipates “energy” in its oscillatory behavior (where energy is to be understood as the integral along  $x$  of the right-hand side of Equation 14; see Jordan & Smith, 1977, and Footnote 1). In another vein, it should be recognized that the model’s dynamics are entirely deterministic in their present form. Stochastic processes, which have been shown quite recently to play a crucial role in effecting movement transitions (Kelso & Scholz, 1985; Kelso, Scholz, & Schöner, 1986; Schöner et al., 1986), have not been considered. However, these processes are probably present, as evidenced, for example, in the scatter of amplitudes at a given oscillation frequency. Stochastic properties of rhythmic movement patterns may be ex-

pored independent of perturbation experiments by appropriate spectral analysis of the time-series data (see, e.g., Kelso & Scholz, 1985). Elaboration of the model to incorporate stochastic aspects is warranted and is a goal of further research.

A final comment concerns the physiological underpinnings of our behavioral results. With respect to the present model, such underpinnings are obscure at the moment. Just as there are many mechanisms that can achieve macroscopic ends, so too there are many mechanisms that can instantiate limit cycle behavior (for a brief discussion, see Kelso & Tuller, 1984, pp. 334–338). The aim here has been to create a model that can realize the stability and reproducibility of certain so-called “simple” movement behaviors. Whatever the physiological bases of the latter, our argument is that they must be consistent with low-dimensional dissipative dynamics. There is not necessarily a dichotomy between the present macroscopic account, which stresses kinematic properties as emergent consequences of an abstract dynamical system, and a more reductionistic approach, which seeks to explain macrophenomena on the basis of microscopic properties. The basis for explanation of a complex phenomenon like movement may be the same (i.e., dynamical) at all levels within the system, operative, perhaps, on different time scales.

## References

- Asatryan, D. G., & Feldman, A. G. (1965). Functional tuning of the nervous system with control of movement or maintenance of a steady posture: I. Mechanographic analysis on the work of the joint on execution of a postural task. *Biophysics*, *10*, 925–935.
- Berkenblit, M. B., Feldman, A. G., & Fukson, O. I. (1986). Adaptability of innate motor patterns and motor control mechanisms. *Behavioral and Brain Sciences*, *9*, 585–638.
- Bizzi, E., & Abend, W. (1983). Posture control and trajectory formation in single and multiple joint arm movements. In J. E. Desmedt (Ed.), *Brain and spinal mechanisms of movement control in man*. (pp. 31–45) New York: Raven.
- Bizzi, E., Polit, A., & Morasso, P. (1976). Mechanisms underlying achievement of final head position. *Journal of Neurophysiology*, *39*, 435–444.
- Brooks, V. B. (1979). Motor programs revisited. In R. E. Talbot & D. R. Humphrey (Eds.), *Posture and movement* (pp. 13–49). New York: Raven.
- Conrad, B., & Brooks, V. B. (1974). Effects of dentate cooling on rapid alternating arm movements. *Journal of Neurophysiology*, *37*, 792–804.
- Cooke, J. D. (1980). The organization of simple, skilled movements. In G. E. Stelmach & J. Requin (Eds.), *Tutorials in motor behavior* (pp. 199–212). Amsterdam: North-Holland.
- Craik, K. J. W. (1947a). Theory of the human operator in control systems: I. The operator as an engineering system. *British Journal of Psychology*, *38*, 56–61.
- Craik, K. J. W. (1947b). Theory of the human operator in control systems: II. Man as an element in a control system. *British Journal of Psychology*, *38*, 142–148.
- Davis, W. E., & Kelso, J. A. S. (1982). Analysis of invariant characteristics in the motor control of Down's syndrome and normal subjects. *Journal of Motor Behavior*, *14*, 194–212.
- Feldman, A. G. (1966). Functional tuning of the nervous system with control of movement or maintenance of a steady posture: III. Mechanographic analysis of execution by man of the simplest motor tasks. *Biophysics*, *11*, 766–775.
- Feldman, A. G. (1980). Superposition of motor programs: I. Rhythmic forearm movements in man. *Neuroscience*, *5*, 81–90.
- Feldman, A. G. (1986). Once more on the equilibrium point hypothesis. *Journal of Motor Behavior*, *18*, 17–54.
- Fitts, P. M. (1954). The information capacity of the human motor system in controlling the amplitude of movement. *Journal of Experimental Psychology*, *47*, 381–391.
- Freund, H.-J. (1983). Motor unit and muscle activity in voluntary motor control. *Physiological Reviews*, *63*, 387–436.
- Haken, H. (1975). Cooperative phenomena in systems far from thermal equilibrium and in nonphysical systems. *Review of Modern Physics*, *47*, 67–121.
- Haken, H. (1983). *Advanced synergetics*. Heidelberg: Springer-Verlag.
- Haken, H. (1985). *Laser light dynamics*. Amsterdam: North-Holland.
- Haken, H., Kelso, J. A. S., & Bunz, H. (1985). A theoretical model of phase transitions in human hand movements. *Biological Cybernetics*, *51*, 347–356.
- Hollerbach, J. (1981). An oscillator theory of handwriting. *Biological Cybernetics*, *39*, 139–156.
- Hogan, N. (1985). Control strategies for complex movements derived from physical systems theory. In H. Haken (Ed.), *Complex systems: Operational approaches in neurobiology, physics, and computers* (pp. 156–168) Heidelberg: Springer-Verlag.
- Holt, E. von (1973). On the nature of order in the central nervous system. In *The behavioral physiology of animals and man: The collected papers of Erich von Holst* (pp. 3–32). Coral Gables, FL: University of Miami Press. (Original work published 1937)
- Hoyt, D. F., & Taylor, C. R. (1981). Gait and the energetics of locomotion in horses. *Nature*, *292*, 239–240.
- Jeannerod, M. (1984). The timing of natural prehensile movements. *Journal of Motor Behavior*, *16*, 235–254.
- Jordan, D. W., & Smith, P. (1977). *Nonlinear ordinary differential equations*. Oxford: Clarendon Press.
- Katz, D. (1948). *Gestaltpsychologie* [Gestalt psychology]. Basel: Schwabe.
- Kay, B., Munhall, K. G., Vatikiotis-Bateson, E., & Kelso, J. A. S. (1985). A note on processing kinematic data: Sampling, filtering, and differentiation. *Haskins Laboratories Status Report on Speech Research*, *SR-81*, 291–303.
- Kelso, J. A. S. (1977). Motor control mechanisms underlying human movement reproduction. *Journal of Experimental Psychology: Human Perception and Performance*, *3*, 529–543.
- Kelso, J. A. S. (1981). On the oscillatory basis of movement. *Bulletin of the Psychonomic Society*, *18*, 63.
- Kelso, J. A. S. (1984). Phase transitions and critical behavior in human bimanual coordination. *American Journal of Physiology: Regulatory, Integrative, and Comparative*, *246*, R1000–R1004.
- Kelso, J. A. S., & Holt, K. G. (1980). Exploring a vibratory systems analysis of human movement production. *Journal of Neurophysiology*, *43*, 1183–1196.
- Kelso, J. A. S., Holt, K. G., Kugler, P. N., & Turvey, M. T. (1980). On the concept of coordinative structures as dissipative structures: II. Empirical lines of convergence. In G. E. Stelmach & J. Requin (Eds.), *Tutorials in motor behavior* (pp. 49–70). New York: North-Holland.
- Kelso, J. A. S., Holt, K. G., Rubin, P., & Kugler, P. N. (1981). Patterns of human interlimb coordination emerge from the properties of nonlinear limit cycle oscillatory processes: Theory and data. *Journal of Motor Behavior*, *13*, 226–261.
- Kelso, J. A. S., & Kay, B. (in press). Information and control: A macroscopic basis for perception–action coupling. To appear in H. Heuer & A. F. Sanders (Eds.), *Tutorials in perception and action*. Hillsdale, N.J.: Erlbaum.
- Kelso, J. A. S., & Scholz, J. P. (1985). Cooperative phenomena in biological motion. In H. Haken (Ed.), *Complex systems: Operational ap-*

- proaches in neurobiology, physics, and computers* (pp. 124–149). New York: Springer-Verlag.
- Kelso, J. A. S., Scholz, J. P., & Schöner, G. (1986). Nonequilibrium phase transitions in coordinated biological motion: Critical fluctuations. *Physics Letters A*, *118*, 279–284.
- Kelso, J. A. S., Schöner, G., Scholz, J. P., & Haken, H. (1987). Phase-locked modes, phase transitions and component oscillators in biological motion. *Physica Scripta*, *5*, 79–87.
- Kelso, J. A. S., Southard, D. L., & Goodman, D. (1979). On the coordination of two-handed movements. *Journal of Experimental Psychology: Human Perception and Performance*, *5*, 229–238.
- Kelso, J. A. S., & Tuller, B. (1984). A dynamical basis for action systems. In M. S. Gazzaniga (Ed.), *Handbook of cognitive neuroscience* (pp. 321–356). New York: Plenum.
- Kelso, J. A. S., & Tuller, B. (1985). Intrinsic time in speech production: Theory, methodology, and preliminary observations. *Haskins Laboratories Status Report on Speech Research, SR-81*, 23–39. Also (in press) in E. Keller & M. Gopnik (Eds.), *Sensory and motor processes in language*. Hillsdale, NJ: Erlbaum.
- Kelso, J. A. S., Tuller, B., Vatikiotis-Bateson, E., & Fowler, C. A. (1984). Functionally specific articulatory cooperation following jaw perturbation during speech: Evidence for coordinative structures. *Journal of Experimental Psychology: Human Perception and Performance*, *10*, 812–832.
- Kelso, J. A. S., Vatikiotis-Bateson, E., Saltzman, E. L., & Kay, B. (1985). A qualitative dynamic analysis of reiterant speech production: Phase portraits, kinematics, and dynamic modeling. *Journal of the Acoustical Society of America*, *77*, 266–280.
- Kent, R. D., & Moll, K. L. (1972). Cinefluorographic analyses of selected lingual consonants. *Journal of Speech and Hearing Research*, *15*, 453–473.
- Kugler, P. N., Kelso, J. A. S., & Turvey, M. T. (1980). On the concept of coordinative structures as dissipative structures: I. Theoretical lines of convergence. In G. E. Stelmach & J. Requin (Eds.), *Tutorials in motor behavior* (pp. 3–47). New York: North-Holland.
- MacKenzie, C. L., & Patla, A. E. (1983). Breakdown in rapid bimanual finger tapping as a function of orientation and phasing. *Society for Neuroscience* (Abstract).
- Maxwell, J. C. (1952). *Matter and motion*. New York: Dover. (Original work published 1877)
- Meyer, D. E., Smith, J. E., & Wright, C. E. (1982). Models for speed and accuracy of aimed movements. *Psychological Review*, *89*, 449–482.
- Minorsky, N. (1962). *Nonlinear oscillations*. Princeton, NJ: Van Nostrand.
- Ostry, D. J., & Munhall, K. (1985). Control of rate and duration in speech. *Journal of the Acoustical Society of America*, *77*, 640–648.
- Polit, A., & Bizzi, E. (1978). Processes controlling arm movements in monkeys. *Science*, *201*, 1235–1237.
- Rayleigh, Baron (John William Strutt). (1945). *Theory of sound* (Vol. 1). New York: Dover. (Original work published 1877)
- Saltzman, E. L., & Kelso, J. A. S. (1987). Skilled actions: A task dynamic approach. *Psychological Review*, *94*, 84–106.
- Schmidt, R. A. (1985, November). “Motor” and “action” perspectives on motor behavior: Some important differences, mainly common ground. Paper presented at the conference entitled “Perspectives on Motor Behavior and Control” at the Zentrum für interdisziplinäre Forschung (Center for Interdisciplinary Research), Universität Bielefeld, West Germany.
- Schmidt, R. A., & McGown, C. (1980). Terminal accuracy of unexpectedly loaded rapid movements: Evidence for a mass–spring mechanism in programming. *Journal of Motor Behavior*, *12*, 149–161.
- Schmidt, R. A., Zelaznik, H. N., Hawkins, B., Frank, J. S., & Quinn, J. T., Jr. (1979). Motor-output variability: A theory for the accuracy of rapid motor acts. *Psychological Review*, *86*, 415–451.
- Schöner, G., Haken, H., & Kelso, J. A. S. (1986). A stochastic theory of phase transitions in human hand movements. *Biological Cybernetics*, *53*, 247–257.
- Scripture, E. W. (1899). Observations of rhythmic action. *Studies from the Yale Psychological Laboratory*, *7*, 102–108.
- Stetson, R. H., & Bouman, H. D. (1935). The coordination of simple skilled movements. *Archives de Néerlandaises de l'Homme et des Animaux*, *20*, 179–254.
- Tuller, B., & Kelso, J. A. S. (1985, November). Bimanual coordination following commissurotomy. Paper presented at the meeting of the Psychonomic Society, Boston, MA.
- Viviani, P., & McCollum, G. (1983). The relation between linear extent and velocity in drawing movements. *Neuroscience*, *10*, 211–218.
- Viviani, P., Soechting, J. F., & Terzuolo, C. A. (1976). Influence of mechanical properties on the relation between EMG activity and torque. *Journal of Physiology* (Paris), *72*, 45–52.
- Viviani, P., & Terzuolo, V. (1980). Space–time invariance in learned motor skills. In G. E. Stelmach & J. Requin (Eds.), *Tutorials in motor behavior* (pp. 525–533). Amsterdam: North-Holland.
- van der Pol, B. (1922). On oscillation hysteresis in a triode generator with two degrees of freedom. *Philosophical Magazine*, *43*, 700–719.
- Winfree, A. T. (1980). *The geometry of biological time*. New York: Springer-Verlag.
- Yamanishi, J., Kawato, M., & Suzuki, R. (1979). Studies on human finger tapping neural networks by phase transition curves. *Biological Cybernetics*, *33*, 199–208.
- Yamanishi, J., Kawato, M., & Suzuki, R. (1980). Two coupled oscillators as a model for the coordinated finger tapping by both hands. *Biological Cybernetics*, *37*, 219–225.

## Appendix A

## Limit Cycle Model Calculations

In this appendix we illustrate some of the basic tools employed in the model calculations in terms of the van der Pol oscillator. For an introduction to such techniques see, for example, Haken (1983), Jordan and Smith (1977), and Minorsky (1962).

The equation of motion of the van der Pol oscillator is again

$$\ddot{x} + \alpha\dot{x} + \gamma x^2\dot{x} + \omega^2 x = 0. \quad (\text{A1})$$

For small nonlinearity this is very close to a simple harmonic oscillator of frequency  $\omega$ . The idea here is that the nonlinearity stabilizes the oscillation at a frequency not too different from  $\omega$ . This suggests a transformation from  $x(t)$  and  $\dot{x}(t)$  to new variables, namely, an amplitude  $r(t)$  and phase  $\phi(t)$  ( $x(t) = 2r(t)\cos[\omega t + \phi(t)]$ ). For ease of computation, we adopt complex notation

$$x = B(t)e^{i\omega t} + B^*(t)e^{-i\omega t}, \quad (\text{A2})$$

where  $B$  is a complex time dependent amplitude and  $B^*$  is its complex conjugate. In this new coordinate system we can define two important approximations to the exact solution (which is unobtainable analytically). The slowly varying amplitude approximation amounts to assuming  $|B| \ll \omega B$  and is used in a self-consistent manner (see below). The rotating wave approximation (RWA) consists of neglecting terms higher in frequency than the fundamental, such as  $e^{3i\omega t}$ ,  $e^{-3i\omega t}$ , and so forth. This means that the anharmonicity of the solution is neglected (this is why the RWA is sometimes also called the *harmonic balance approximation*). See, for example, Haken (1985) for a physical interpretation of these approximations. Using Equation A1 and these two approximations we obtain for Equation A1

$$B = -\frac{\alpha B}{2} - \frac{\gamma|B|^2 B}{2}. \quad (\text{A3})$$

Introducing polar coordinates in the complex plane,

$$B(t) = r(t)e^{i\phi(t)}, \quad (\text{A4})$$

and separating real and imaginary parts we find

$$\dot{r} = -\frac{\alpha r}{2} - \frac{\gamma r^3}{2} \quad (\text{A5})$$

$$\dot{\phi} = 0. \quad (\text{A6})$$

Equation A5 for the radius  $r$  of the limit cycle (which here is a limit circle in the complex plane due to the RWA) has a form that makes visualization of its solutions very simple—namely, it corresponds to the overdamped movement of a particle in the potential:

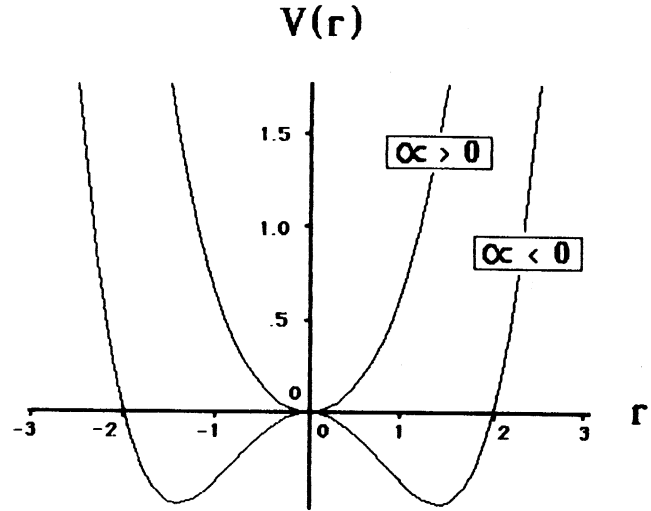


Figure A1. Amplitude potential,  $V$ , as a function of the amplitude,  $r$ , for the van der Pol oscillator, when  $\alpha$  is less than zero and greater than zero. (Units are arbitrary [see Appendix B].)

$$V(r) = \frac{\alpha r^2}{4} + \frac{\gamma r^4}{8}. \quad (\text{A7})$$

This potential is illustrated in Figure A1 for  $\alpha > 0$  and for  $\alpha < 0$ , while  $\gamma > 0$  in both cases.

Obviously for  $\gamma > 0$ , the limit cycle of finite amplitude,

$$r_0 = \sqrt{|\alpha|/\gamma}, \quad (\text{A8})$$

is a stable, stationary solution. A movement with an amplitude close to  $r_0$  relaxes to the limit cycle according to

$$r(t) = (r(t=0) - r_0)e^{-\alpha t} + r_0 \quad (\text{A9})$$

(as can be seen by linearization of Equation A5 around  $r = r_0$ ). Thus this amplitude varies slowly, as long as  $|\alpha| \ll \omega$ . This is the above-mentioned self-consistency condition. The time  $(1/|\alpha|)$  is called the relaxation time of the amplitude. Equation A6 of the relative phase shows that phase is marginally stable, that is, does not return to an initial value if perturbed. This can be tested in phase resetting experiments as explained in the General Discussion.

## Appendix B

## Dimensional Analysis of Hybrid, Nonlinear Oscillator

Here we perform a dimensional analysis to compare different contributions to the oscillator dynamics. To that end we estimate the different forces in the equation of motion (Equation 5) by their amplitudes when the system is on the limit cycle. The linear restoring force behaves as

$$\omega^2 x \approx \omega^2 r_0, \quad (\text{B1})$$

where  $r_0$  is the radius of the limit cycle. The linear (negative) damping is

$$\alpha \dot{x} \approx \alpha \omega r_0. \quad (\text{B2})$$

The van der Pol nonlinearity is

$$\gamma x^2 \dot{x} \approx \gamma \omega r_0^3, \quad (\text{B3})$$

while the Rayleigh nonlinearity scales as

$$\beta \dot{x}^3 \approx \beta \omega^3 r_0^3. \quad (\text{B4})$$

Using Equation 6,

$$r_0 = 2\sqrt{|\alpha|/(3\beta\omega^2 + \gamma)}$$

as the radius of the hybrid limit cycle, the strength of the nonlinear dissipative terms relative to the linear restoring term is

$$\frac{\beta \dot{x}^3 + \gamma x^2 \dot{x}}{\omega^2 x} \approx \frac{\alpha(\beta\omega^2 + \gamma)}{\omega(3\beta\omega^2 + \gamma)}. \quad (\text{B5})$$

For either of the simple oscillators this reduces to  $\alpha/\omega$ .

Received March 17, 1986

Revision received August 15, 1986 ■